IEEE Access
Multidisciplinary | Rapid Review | Open Access Journal

Received May 28, 2020, accepted June 9, 2020, date of publication June 22, 2020, date of current version July 20, 2020.

Digital Object Identifier 10.1109/ACCESS.2020.3004067

Adaptive Tuning of Power System Stabilizer Using a Damping Control Strategy Considering Stochastic Time Delay

JOSÉ ANTONIO OSCULLO LALA[1], (Student Member, IEEE), AND CARLOS FABIAN GALLARDO[1]

Electrical Engineering Department, Faculty Electricity and Electronic, National Polytechnic School, Quito 170525, Ecuador

Corresponding author: José Antonio Oscullo Lala (jose.oscullo@epn.edu.ec)

This work was supported by the Escuela Politécnica Nacional, through the research funds of the Vicerrectorado de Investigación y Proyección Social.

ABSTRACT The operation of a modern electrical system presents complex operating conditions, and uncertainty factors increased by the presence of variable and flexible loads. This stochastic operating point variation can promote low-frequency oscillations, and like the conventional power system stabilizer (PSS) features static tuning, it does not provide sufficient damping. Today, an electrical system is monitored through online measurements from the wide-area measurement system (WAMS); moreover, it enables stochastic dynamics to be tracked as the remote signals of WAMS system, the time delay due to the communication channel. It is interesting to analyze the incorporation of the PSS of signals from the WAMS without the time delay effect that degrades the small-signal stability (SSS) and, in turn, allows adaptive tuning. Through two stages, at first, the subspace of the operating point is determined based on a distribution of consumption levels. Each operating point considered a random time delay. For each subspace, establish a bank of tuned PSSs. Second, through the optimal classification and the regression decision tree (CART), the classification rules for the subspace are determined, allowing classifying the measurements of WAMS. The proposed methodology is applied to the New England of 66-bus system and Ecuadorian electric system to demonstrate that the adaptive tuning of PSSs significantly improves SSS under different scenarios and is probabilistic robust, considering the time delay.

INDEX TERMS Stochastic power system operating, power oscillations, adaptive damping control, swarm intelligence algorithms, wide area damping controller.

I. INTRODUCTION

System electric power (SEP) currently has large regional grids with different types of flexible and variable loads, generally distant from generation resources. This operational situation determines the presence of low-frequency oscillations in the interconnections of areas, a situation that limits the transfer of energy flow between them. The SSS analysis determines SEP ability to maintain synchronism under small disturbances.

Given the operation of the system, many uncertainty factors affect SSS. For example, there is a deviation in the control adjustment parameters due to the generators' dynamics, load change, network parameters, the energy exchange between different areas of the system, etc. Therefore, the model of a conventional PSS, by not being able to observe these factors that cause low-frequency oscillations, can compromise the damping of oscillations or worsen the stability of the system [1], [2].

As the SSS level is defined by the damping percentage of the low-frequency oscillation modes in this way since the most effective and economical way to restrict low-frequency oscillation is through the installation of PSSs [3]. In most systems, conventionally, the PSS uses the generator speed as the local power signal that allows a reasonable operation to damp the low-frequency oscillations using fixed parameters obtained for one operating condition by different techniques [4].

The associate editor coordinating the review of this manuscript and approving it for publication was Siqi Bu.

Today, the phasor measurement unit (PMU) is a requirement for the entry of new system installations. Through which real-time monitoring of system dynamics is possible, and together with advanced algorithms for processing measurements at various points of the power system, it is possible to determine the oscillatory behavior after an event or disturbance. This system, called WAMS, has the signals transmitted through a communication channel.

These signals have high observability of the modes swings between areas that can serve as feedback in the PSSs to improve the SSS of the power system significantly [5]. However, the WAMS signals contain a delay of a few milliseconds due to the type of communication channel, which consequently can severely degrade the SSS.

Thus, stability analysis constitutes a probabilistic problem rather than a deterministic one. Due to system factors, the disturbances in conjunction with the operating conditions of the system are stochastic. In addition, the communication delay, several other power system parameters have an undesirable effect on SSS [6].

In [7], an analysis of SSS is showed by considering the stochasticity of the time delay of PMU signals that feed the POD of wind or solar generation units, which are parameterized by using swarm intelligence algorithm techniques through of accumulated probabilistic method.

Now in [8], the expected value method (as known as expectation model) of the system eigenvalues is used through the probabilistic analysis on the time delay variable of the exchange power obtained by PMUs, where it is shown that an adequate adjustment of the PSS gain allows limiting the effect of the time delay by improving the SSS.

In [9], present the application of predictive control to frequency control between two areas based on scenario analysis. Still, if the operating conditions change over a wide range, the robustness of the control may not be ensured. Therefore, adaptive control methods such as the fuzzy control method [10], [11], the combination of linearized models for each point real operation system, in which the design for each model an observer-based state feedback controller a priori to reach a specified performance objective [12]. Another approach that was developed with the Kalman filter method and compare with the method classification and regression tree (CART) is a very popular decision tree (DTs) as an intelligent classifiers method. It builds extreme system operating points, and it establishes polytopes for damping inter-area oscillations with FACTS to base on sensing and classify the current of the operating lines. The CART is a non-parametric DTs learning technique for adaptive selecting the controllers appropriate. Still, in the presence of common vertices, the accuracy of that method was found to suffer [13].

Nonetheless, as the operating conditions change considerably, the nonlinearity of electrical systems is more outstanding, and the disturbances can present oscillations that are not easy to interpret [14]. This situation is performed for a random variation of load for designing an adaptive damping controller for tracking the difference. Consequently, a can be analyzed using machine learning methods, where statistical analysis can be used to determine the characteristics of big data through CART [15]. The problem is that the load analysis scenario is addressed in [16] for robustly deciding to select the PSS parameters for neural-like P systems optimization.

Therefore, tuning of the parameters of PSSs has been investigated. The generality is analyzed considering a particular operational scenario, due to the difficulty in which the PSS parameters adapt to changes in conditions once they are established. When is considering the randomness of wind energy, a tuning scheme of PSSs is presented in [7]. Through the establishment of a composition of the cumulative distribution functions for damping and frequency error of the mode of interest concerning the operation without PSSs will have determined related to the generated of wind power and the activity with conventional PSSs ubicated by the highest residue.

Therefore, improving the observability of PSS employing an additional signal, through which it is possible to damp the low-frequency oscillation considering the time delay and the load condition of the system. This situation allows using the existing infrastructure of PSSs, and the measurements of WAMS to time have not yet analyzed. In this document, we consider the uncertainty in the load, which can be due to several factors, such as the economic, demographic, daily, or seasonal load cycle. Additionally, due to the device electronics, there are flexible loads and time delays, which constitute a high risk for low-frequency oscillatory stability.

This paper is organized as follows: Section 2 presents the different methodologies and tools considered for the modeling and control of the electrical system. Section 3 contains the proposal methodological that allows achieving the damping of the oscillations for the multi-machine and multi-scenario system. Section 4 presents the characteristic of the test system and the main results with its analysis. Finally, section 5 presents the conclusions of the study.

II. ADAPTIVE DAMPING CONTROL SCHEME BASED ON CART

The CART is one of the classification machine learning algorithms, through which the recursive partition of the set of data into different subspaces is made. It based on the variables of interest. Thus, creating classification and regression trees. The classification trees allow determining the partition rules of each subspace. With the regression trees, it is possible to identify to which subspace the analyzed operating point of the system corresponds.

A. BUILDING SUBSPACES

The daily operation of an electrical system due to load variation establishes a variation operating condition, with a lower and upper limit. Fig. 1 shows the division into intervals in which several subspaces (E_i) are constructed that together are equivalent to the current operating condition. Each subspace has a set rule, those are determined, and the data can belong to a specific subspace. Since the simulation, it is possible to

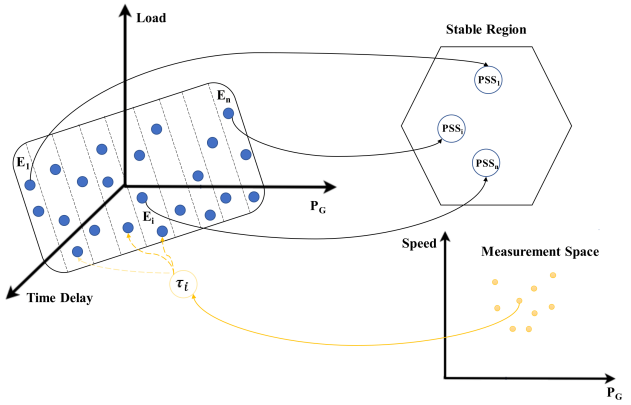

FIGURE 1. Construction of subspaces for parameter space and measurement space.

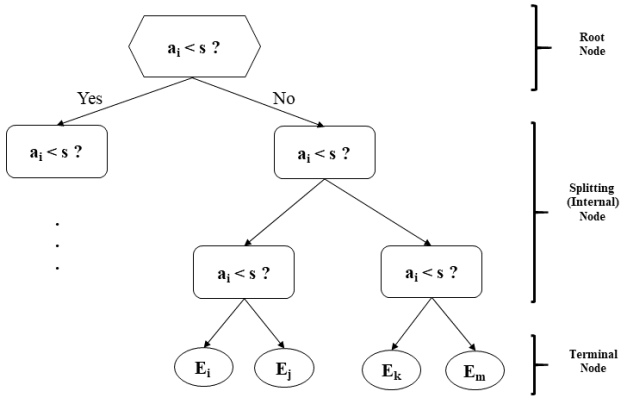

FIGURE 2. Typical structure of CART.

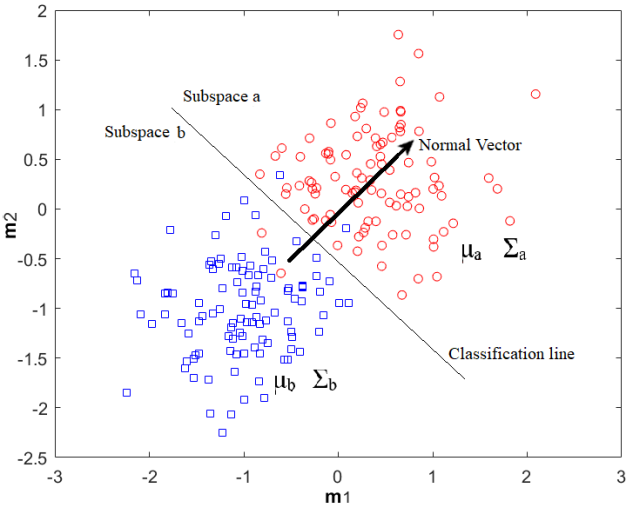

FIGURE 3. Classifying the two different subspaces for conditions operating.

classify the subspaces of the current operating point. However, in case of identification of the subspace of system data, WAMS that contains a time delay is set by regression.

This feature of subspaces allows adjusting to multiple operating conditions of the system. The analysis of each subspace establishes a requirement for the selection, location, and adjustment parameters of PSS through modal analysis that identifies the oscillation modes. Since PMUs monitor the bus's frequency and power in operating conditions, they would be used to control the power grid through the optimal online tuning of the parameters.

B. THE CART HOW ADAPTIVE CONTROL SCHEME

The multiple operative conditions of a large-scale electrical system cannot be adequately characterized in a subspace by a single measurement. Therefore, various measures must be used to track the variation of the operating point of the power system. In this way, PSSs can be pre-tuned offline using multiple operating conditions and can be adaptive switched using online measurements. As the load fluctuates, the operating system point will deviate from the initial subspace moving randomly to other operating subspaces or return to the initial subspace. Thus, the CART allows identifying the subspace of interest to determine which PSSs are connected online. The measurements of all the subspaces of the operating points make up the learning set, which is the CART input data.

The CART is built from top to bottom and consists of a root node, internal nodes, and terminal nodes. The root node and each internal node establish two subnodes with incoming branches and outgoing branches employing an optimal division rule, based on a potential division value (s) of an attribute (a), where a subset of the learning data set is selected, while a terminal node is a pure node that could not be further divided, as presented in Fig. 2.

The classification process in the CART starts from the top root node, and at each level, the subsets will be divided according to the optimal division rules. The division rules are of the form "if-then" For the case study in this document, each terminal node represents a subspace of the operating condition. Additional details on the CART algorithm in [17] provide a complete introduction to the general DTs theory.

In the case of tuning the PSSs, the speed of the generators is generally used, since this variable indirectly has information on the level of power input, topology and the oscillation modes of the generator concerning the electrical system. However, this variable is generally not available in PMUs. Still, the generator bus frequency is available, which is a function of the angle of the external bus of the generators so that it will be used in the data set of learning.

Since the learning data set contains multiple measurements in each subspace makes the classification process complex. Therefore, to differentiate the measurement characteristics in different subspaces, the Euclidean distance to the hyperplanes is used as a classification parameter to process large amounts of measurement data. In Fig. 3, the measurements of subspaces a and b in circles and squares, respectively, are presented for the ease of a two-dimensional space, and the analysis is similar for the case of a space of n dimensions when there are n measurements. Utilizing a classification

line, two groups of data (subspaces) are distinguished, and in the three-dimensional case, a plane is required. By having multiple measurements, as in the case of the electrical system, a flat hyper-plane is used to distinguish the subspaces at the operating points.

In each group, the mean μ and the covariance Σ of the measurements of subspaces a and b, respectively, can be obtained. The optimal division into different operational classes using multiple measures is established by the classification line, in which the normal vector W to the hyper-plane, allows creating the classification rule of two data classes through the relationship of the variance between the class to variance within categories such as (1), which is called Fisher's linear discriminant which maximizes the difference between the classes [18].

$$\mathbb{S} = \frac{(W^T(\mu_a - \mu_b))^2}{W^T(\sum_a + \sum_b)W}. \tag{1}$$

Be the maximum value of (1) when the normal vector is determined as in (2).

$$W_m = (\Sigma_a + \Sigma_b)^{-1}(\mu_a - \mu_b). \tag{2}$$

In the same way, the optimal classification line is determined with the maximum normal vector W_m and the midpoint of the means of each group (μ_m), as in (3).

$$\mu_m = \frac{\mu_a + \mu_b}{2}. \tag{3}$$

Now it is possible to determine the distance from any point of operation to the hyper-plane. For the multiple dimensional cases, the normal vector of a hyper-plane can also be calculated by (1). The hyper-plane γ is established through of vector comprising of operating points ϕ concerning the midpoints of each group, as in (4).

$$\gamma : W.(\phi - \mu_m) = 0. \tag{4}$$

The distance vector of the points of the subspaces $\phi_i = (x_i, y_i, z_i, \ldots)$ to the hyper-plane γ can be obtained as in (5). For the two-dimensional case, if $d_i \geq 0$, it is identified that the operating point is within the subspace a; otherwise, the point a is within subspace b.

$$d_i = \frac{W.(\phi_i - \mu_m)}{\|W\|}. \tag{5}$$

where d_i is the input variable for the CART employing which the classification process is carried out to determine the rules for dividing subspaces, by establishing the rules, the regression process can be carried out, with which it is possible to identify the subspace to which the analyzed operating point belongs. In this way, the CART algorithm can track the variation system operating point's in the subspaces and guide the updating of the PSSs required by the operating conditions in an adaptive way.

III. MODEL OF POWER SYSTEM UNCERTAINTIES AND DATA SET

A. DESIGN OF PSS

For each operative subspace, the tuning parameters of the adequately coordinated PSSs are determined to use a heuristic algorithm to ensure that the operative point of the system is within the stable region. In the study, residues will be used to determine the location for activation of PSSs to tune; consequently, this increases the limits of small-signal stability.

Fig. 4 shows the type of PSS modeled, in which the speed and power of the generator are used as input signals to the time delay compensator (DC), taking advantage of the ease of measuring them. However, when the oscillations present great and intermittent changes in power, they can be registered in the PSS, creating an unwanted output signal, a situation that determines the need to have limits for these cases and achieves the adaptability of the response in the PSS to changes in the generator's operating point.

The outputs that feed a conventional PSS structure, so it was stated in [19], thereby improving SSS. The delay of the control signals causes a controller to perform an action based not on the system's updated operating condition. That is, the signal received by the PSS does not correspond to the operating point, which can affect the stability of the system, so it should be eliminated the phase delay caused by the delay in signal communication, and since the delay time is a variable trying to control it considering only the lower and upper limits could lead to an unwanted PSS response. Therefore, it is proposed to analyze it stochastically to consider reality.

B. PROBABILISTIC MODEL OF TIME DELAY

The delay time in WAMS depends on different factors, like the location of the PMU units, the class of communication links, the reliability of the communication link that exhibits stochastic behavior [15].

In reference [20], a theorem is established to transform the rapid changes present in periodic delays into distributed delays; these are treated in [21], through which for a linearized system, it can be represented by equation (6).

$$\dot{x}(t) = A_o x(t) + \sum_{i=1}^{i_{max}} A_i x(t - \tau_i(t)). \tag{6}$$

where $\tau_i(t) : \mathbb{R}^+ \rightarrow [\tau_{min}, \tau_{max}]$, with $0 \leq \tau_{min} < \tau_{max}$.

When the delay presents a rapid change, the small-signal stability can be expressed as in (10). Which is determined, if a specific delay is considered, $\tau_i(t) = \xi$, applying the Laplace transform to (6) such as (7):

$$\mathcal{L}\{\dot{x}(t)\} = A_o \mathcal{L}\{x(t)\} + \sum_{i=1}^{v} A_i \mathcal{L}\{x(t - \xi)\}. \tag{7}$$

For the initial condition xo, apply the Laplace transform to (6). It is established $\mathcal{L}\{\dot{x}(t)\} = sX(s) - x_o$, with $L\{x(t - \xi)\} = e^{-s\xi}X(s)$ for, $t \geq \xi$, and 0 to $t < \xi$, replacing (7) in (6) we have (8):

$$sX(s) - x_o = A_o X(s) + + \sum_{i=1}^{v} A_i e^{-s\xi} X(s). \tag{8}$$

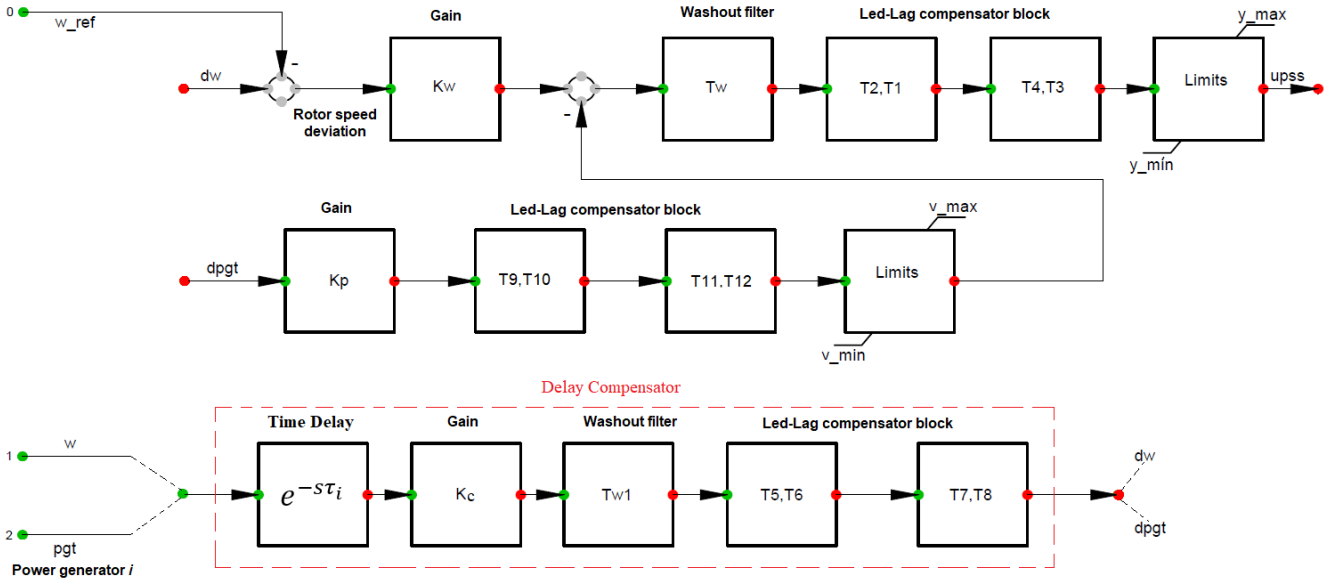

FIGURE 4. Model of PSS

Grouping equation (8) is determined (9), where the term on the right constitutes the characteristic polynomial.

$$(s - A_o - \sum_{i=1}^{v} A_i e^{-s\xi}) X(s) = cI. \quad (9)$$

The same as for the quick change in a specific delay equation (10) is established.

$$\dot{x}(t) = A_o x(t) + \sum_{i=1}^{v} A_i \int_{\tau_{min}}^{\tau_{max}} \omega_i(\xi)\, x(t-\xi)\, d\xi. \quad (10)$$

where:

$$\mathcal{L}\left\{\int_{\tau_{min}}^{\tau_{max}} \omega_i(\xi)\, x(t-\xi)\, d\xi\right\} = \mathcal{L}\{\omega_i(t)\} X(s), \quad (11)$$

with $\mathcal{L}\{\omega_i(t)\} = e^{-s\xi}$, being $\omega_i(\xi)$ the probability density function (PDF) for the specific time delay $\tau_i(t) = \xi$.

In general, the time delay in WAMS presents a behavior of a normal distribution as established [5], but another class of distribution can also be used if historical data is available [22]. The PDF of the time delay for the i-th PSS is set as in (12). Being $\mu_{\tau_i(t)}$ and $\sigma_{\tau_i(t)}$, the mean and standard deviation, respectively, of the time delay.

$$\omega(\tau_i(t)) = \frac{1}{\sigma_{\tau_i(t)}\sqrt{2\pi}} e^{\frac{(\tau_i(t)-\mu_{\tau_i(t)})^2}{2\sigma^2_{\tau_i(t)}}}. \quad (12)$$

Fig. 5 shows the time delay probability density function used in the study, considering an average of 0.5 ms and 0.25 standard deviation. Through these values, it is achieved that PDF for the time delay covers the range of WAMS observed in the actual operation of the electrical systems that are in the range of 0.1 to 0.7 s [7].

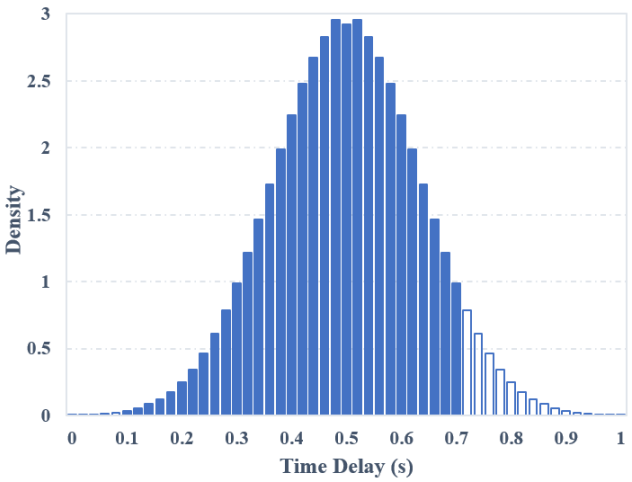

FIGURE 5. A probabilistic model of time delay.

C. PROBABILISTIC MODEL OF OPERATIVE SCENARIO

The system's operating scenario begins by selecting the load condition; in this study, a Gaussian PDF will be used, where the mean and standard deviation are derived from the demand of each bar. Regarding the generation and power grid in a random discrete way, an N-1 contingency is selected. In the case of the study, two parallel circuits of the interconnection lines between the areas are chosen. The output of the generators is carried out by reducing the available number of units of the power plant.

D. DATA SET SELECTION

The data set is selected from the operating condition, and these can be grouped in a matrix way, where m represents the number of subspaces of CART, and n the number of

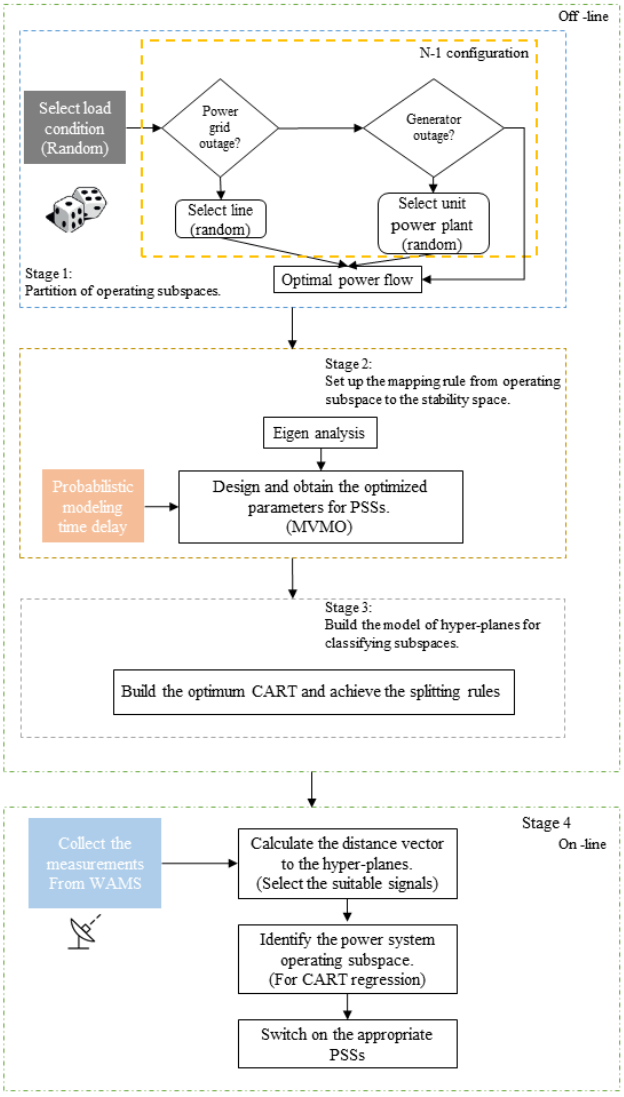

FIGURE 6. Flowchart of implementation of the proposed method to tune the PSSs.

measurements obtained either by simulation or by PMUs. The di is determined from the data set like (5), through which the classification is made across simulation data. It uses of these rules allow us to determine the belonging of a group of data to a subspace by the regression obtained with the CART algorithm.

IV. DESIGN PROCEDURE OF ADAPTIVE PSS CONTROL SCHEME

This paper presents a use that combines CART and tuning of PSSs of an electrical system to maintain the stability of small-signal adaptive to the operating conditions, as shown in Fig. 6. For which four stages. The coordinated tuning process of the PSSs is done offline. The power system's operating space is divided into different operating subspaces according to the stochastic established load condition and time delay in the first stage. In the second stage, for each subspace is determined by eigenanalysis the critical oscillation modes (if it is a viable operating condition obtained through an optimal power flow calculation), and residues. Though they can determine the optimal location of the PSSs, these data are the inputs to the heuristic optimization model used for the study by the well-known Mean-Variance Mapping Optimization (MVMO), to establish a coordinated way the parameters of the PSSs are predesigned in each subspace. In the third stage, the hyper-plans model for classification of subspaces is built, establishing the optimal CART division rules.

The heuristic algorithm MVMO looks for the optimal location and tuning PSSs. Accordingly, calculating the largest residue and damping ratio, respectively, allows it to be accurately parameterized and activated, allowing the damping of multiple conditions operations with critic mode swings and employing the following objective function proposed in (13):

$$\min OF = |\zeta_{min} - \zeta_{sys} \tag{13}$$

$$\zeta_{sys} = \min_{i=1\ldots n} \{ \min_{p=1\ldots k} (\zeta_{ip}) \} \tag{14}$$

$$\text{s.t. } y_{min} \leq y \leq y_{max} \tag{15}$$

where ζ_{min} is the minimum accepted damping ratio (in this document it is established so limit 10%) ζ_{sys} is the minimum damping ratio of the system for each scenario. The vector y represents the solution to the optimization problem, i.e., the different parameters of PSSs (gains and time constants).

The fourth stage is online WAMS information on frequency bus, and the power of generators is chosen as the data set. In which the distance to hyper-plane is calculated and through the rules of division of CART through the regression to which the terminal node of DTs (subspace) of the corresponding operating point, as presented in Fig. 7. Thus, appropriately change the parameters of PSSs according to the CART output, since WAMS allows online sending of remote commands using signal modulation as presented in reference [23]. The situation that is not addressed in this document.

V. RESULTS AND DISCUSSION

A. TEST SYSTEM

The proposed method is illustrated in the New England System modify of 66-bus. The single line diagram of the system is shown in Fig. 8, which is widely used to study small-signal stability. The power plant performs as follows: all generators are thermal, except the generators at buses 1, 2, and 10 that are hydraulic; this allows us to consider the generality of the production sources of an electrical system. The slack bus is assumed to be a bus of B_{3G} generator. It believes that each unit of the power plant has PSSs. The parameters so time constants T_W, T_{W1}, are considered in 10 s. The details about the synchronous generators, line parameters, and load values used in our study are given in [24].

B. SIMULATION RESULTS

For multiple operating conditions established in the study, a load variation of 5% is considered, with a sampling rate of the variables of interest of 60 samples per second for each

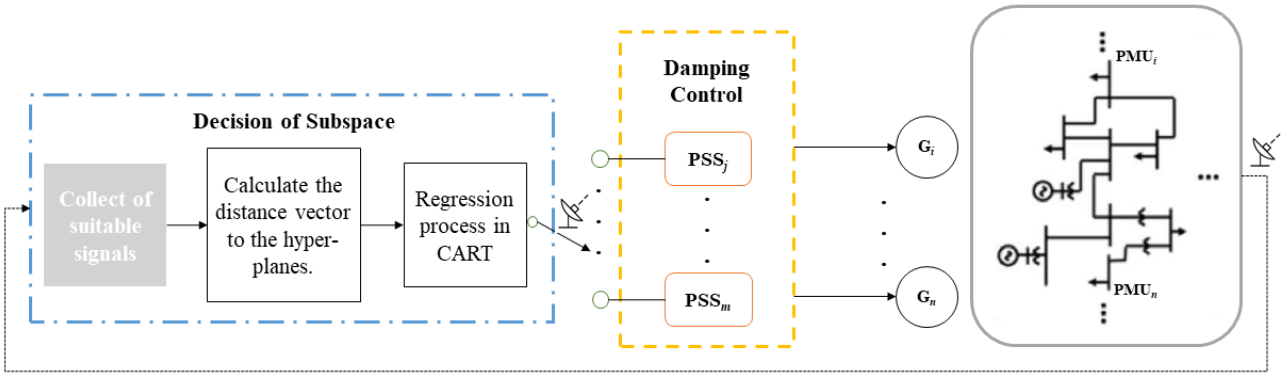

FIGURE 7. Structure of the proposed adaptive damping control scheme.

TABLE 1. Swing modes without PSS.

Subspace	Load Condition (MW)	Mode No.	1	2	3
1	10296	damp. (%)	7.717	-0.067	5.593
		freq. (Hz)	0.841	0.673	0.515
2	10811	damp. (%)	7.775	-0.158	5.541
		freq. (Hz)	0.841	0.674	0.518
3	10910	damp. (%)	7.837	0.596	7.444
		freq. (Hz)	0.841	0.678	0.529
4	11009	damp. (%)	7.852	0.468	7.267
		freq. (Hz)	0.842	0.679	0.531
5	11108	damp. (%)	7.860	0.333	7.075
		freq. (Hz)	0.843	0.679	0.533
6	11207	damp. (%)	7.863	0.198	6.877
		freq. (Hz)	0.844	0.679	0.534
7	11304	damp. (%)	7.857	0.069	6.677
		freq. (Hz)	0.844	0.679	0.535
8	11402	damp. (%)	7.845	-0.053	6.475
		freq. (Hz)	0.845	0.679	0.536
9	11499	damp. (%)	7.826	-0.166	6.271
		freq. (Hz)	0.846	0.678	0.536
10	11595	damp. (%)	7.800	-0.267	6.061
		freq. (Hz)	0.846	0.677	0.536

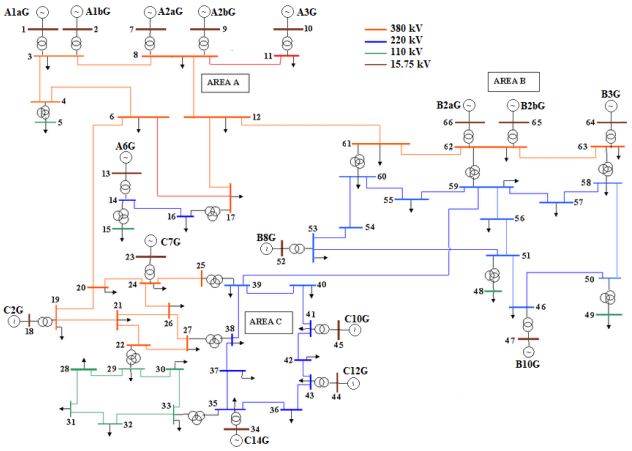

FIGURE 8. New England System 66-bus test system.

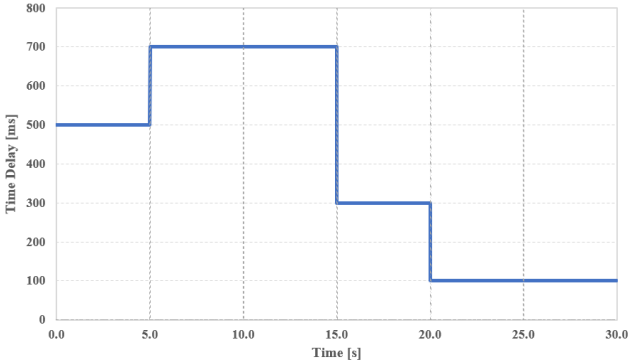

FIGURE 9. Variation of the model of time delay.

subspace. In each subspace through the eigenanalysis, the damping ratio and the frequency of the oscillation modes are determined. Where it is observed how the variation of the operating conditions has an impact on the oscillation modes, as it shows Table 1, it is the possible look that there are three critical modes for each subspace. Critical modes are defined as eigenvalues that have a damping ratio of less than 10%. Being mode 2 in some subspaces, it is in the unstable zone (negative damping). The situation that created to need for the system has a mechanism for updating the parameters of PSSs, through which the system has sufficient damping for each operating condition.

Table 2 shows for each subspace how the critical modes reach a damping ratio over the proposed limit. If considering the activation of DC and time delay stochastic, as shown in Fig. 9, which sufficiently covers the variation of lag time present in the real world in WAMS.

In the off-line stage, the learning set to build the classification tree is generated by 1000 simulations of the test system for each subspace considering the contingency stochastic, and for the case of 10 subspaces, a learning sample of 10,000 is determined CART simulations.

The CART monitors the change of the operating conditions, and since the PSSs are tuned in each subspace off-line, they can be changed to the operating condition of the selected subspace. The measurements used to determine the subspaces with the CART are the frequency of buses. The power of the generator that presents the highest residue. Through which the greatest controllability and observability are sought for each critical oscillation mode, according to so, it is shown in

TABLE 2. Swing modes with PSS.

Subspace	Load Condition (MW)	Mode No.	1	2	3
1	10296	damp. (%)	10.705	10.613	10.538
		freq. (Hz)	0.8466	0.6765	0.5263
2	10811	damp. (%)	10.707	10.708	10.541
		freq. (Hz)	0.8457	0.6746	0.5187
3	10910	damp. (%)	10.807	10.716	10.444
		freq. (Hz)	0.8415	0.6783	0.5291
4	11009	damp. (%)	10.802	10.468	10.267
		freq. (Hz)	0.8424	0.6792	0.5318
5	11108	damp. (%)	10.810	10.333	10.075
		freq. (Hz)	0.8437	0.6791	0.5332
6	11207	damp. (%)	10.803	10.598	10.877
		freq. (Hz)	0.8446	0.6791	0.5343
7	11304	damp. (%)	10.807	10.169	10.677
		freq. (Hz)	0.8449	0.6792	0.5351
8	11402	damp. (%)	10.815	10.064	10.475
		freq. (Hz)	0.8414	0.6792	0.5368
9	11499	damp. (%)	10.827	10.148	10.271
		freq. (Hz)	0.8413	0.6785	0.5363
10	11595	damp. (%)	10.800	10.139	10.061
		freq. (Hz)	0.8416	0.6776	0.5362

TABLE 3. Selection of signals in base of residue.

Subspace	Mode 1		Mode 2		Mode 3	
	Gen.	Residue	Gen.	Residue	Gen.	Residue
1	C_{2G}	0.8791	B_{3G}	0.7858	C_{2G}	0.8792
	C_{7G}	0.1582	A_{2aG}	0.3505	C_{12G}	0.2610
2	C_{2G}	0.8824	B_{3G}	0.7895	C_{2G}	0.8814
	C_{7G}	0.1567	A_{2aG}	0.3506	C_{12G}	0.2736
3	C_{2G}	0.8867	B_{3G}	0.8394	C_{2G}	0.8797
	C_{7G}	0.1609	A_{2aG}	0.3508	C_{12G}	0.2923
4	C_{2G}	0.8907	B_{3G}	0.8379	C_{2G}	0.8896
	C_{7G}	0.2274	A_{2aG}	0.3508	C_{12G}	0.3055
5	C_{2G}	0.8950	B_{3G}	0.8343	C_{2G}	0.8872
	C_{7G}	0.1573	A_{2aG}	0.3508	C_{12G}	0.3177
6	C_{2G}	0.8994	B_{3G}	0.8282	C_{2G}	0.8902
	C_{7G}	0.1557	A_{2aG}	0.3507	C_{12G}	0.3283
7	C_{2G}	0.9041	B_{3G}	0.8196	C_{2G}	0.8952
	C_{7G}	0.1543	A_{2aG}	0.3508	C_{12G}	0.3371
8	C_{2G}	0.9088	B_{3G}	0.8082	C_{2G}	0.9032
	C_{7G}	0.1530	A_{2aG}	0.3507	C_{12G}	0.3438
9	C_{2G}	0.9137	B_{3G}	0.7940	C_{2G}	0.9087
	C_{7G}	0.1520	A_{2aG}	0.3505	C_{12G}	0.2610
10	C_{2G}	0.9186	B_{3G}	0.7769	C_{2G}	0.9175
	C_{7G}	0.1513	A_{2aG}	0.3503	C_{12G}	0.3508

Table 3. Therefore, the measurements used to form the CART correspond to the generators A_{2aG}, B_{3G}, C_{2G}, C_{7G}, and C_{12G}.

Given that, for each subspace, 1000 simulations were considered. It is considering the case of 10 subspaces, the matrix of 10,000 rows by 600 columns is determined as a product of 60 samples by two measurements of five selected generators, a situation that determines that each hyper-plane for classification is formed in a 600-dimensional space for the formation of CART. Since the classification requires two groups and for the case of 10 subspaces, a combinatorial space of 45 hyper-planes is required according to the CART algorithm. And in the regression, to determine the operating subspace, it is necessary to determine the distance to the hyper-plane i-th

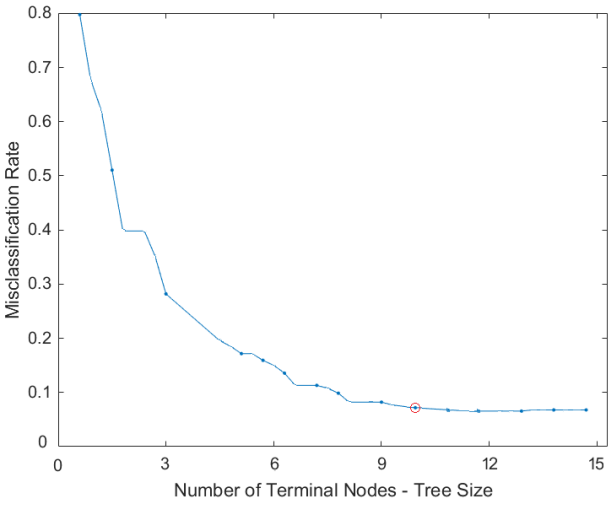

FIGURE 10. The misclassification rate of tree size for the test system.

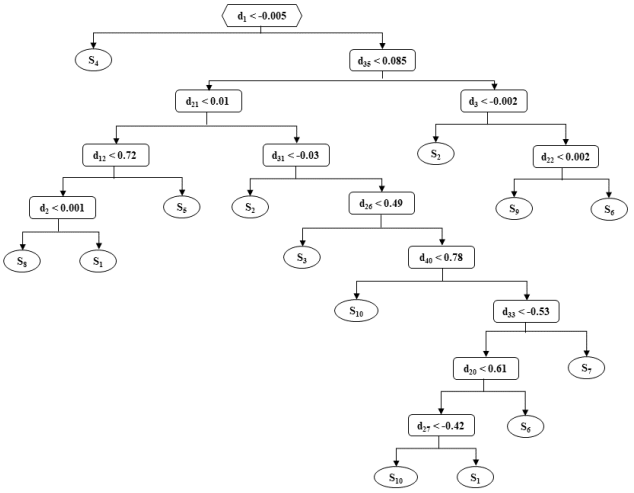

FIGURE 11. Classification of subspace with CART.

that in the case of the ten operating subspaces, it is necessary to have a distance-vector containing 45 distance parameters according to (5).

Therefore, the compromise in the size of the classification tree. If this is of small size, it will not capture the dynamics of the data set's behavior. Large-sized one can lead to an overfit, which can cause an incorrect identification of the subspaces [25]. Therefore, the selection of suitable tree size is based on the classification accuracy in Fig. 10, it is presented that the optimal number of the decision tree for the study is ten subspaces that determine the smallest CART mismatch that reaches 0.0792, representing a 92.1% probability of selecting the correct subspace.

The CART structure is formed for the test system, where the division rules are established in each node, and 10 terminal nodes representing the ten operating subspaces are determined. The classification rule is the distance to the

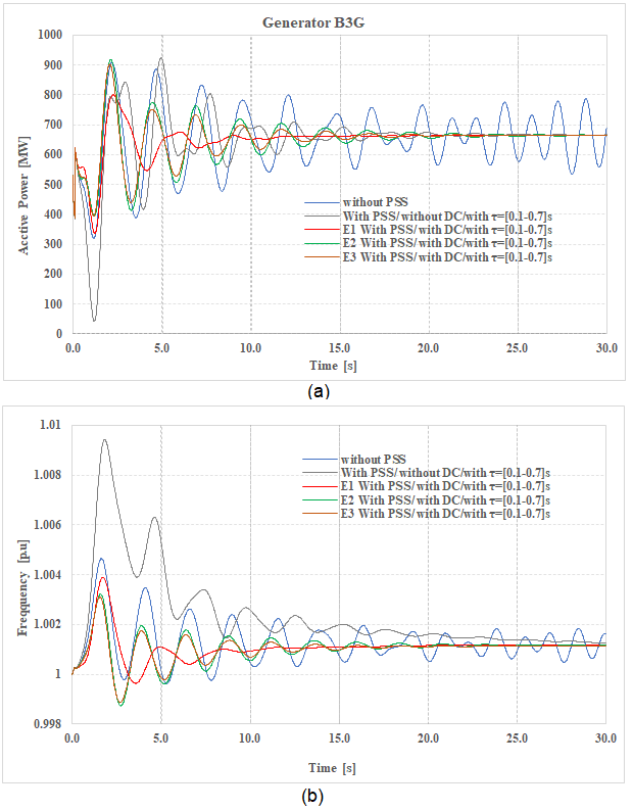

FIGURE 12. Time response of the system under varying time delay in the case of the three subspace boundaries. a) response of slack bus. b) frequency of the system.

hyper-plane according to the parameter calculated, as indicated in section 2, is shown in Fig. 11.

When considering the WAMS data to determine the behavior of regression process, it sees with confusion; the matrix is defined in Table 4, considering for each subspace 5000 different operating points of which there are 354 cases in which they are not adequately classified, which determines a 92.9% accuracy, the declassification points are mainly due to operating points of boundaries between the subspaces.

To determine the robustness of coordination of PSSs considering the operating edges of subspaces, a simulation in the time domain is presented below, regarding the parameterization of PSSs of a subspace concerning of the adjacent subspace, in Fig. 12.

It is observed that the tuning of PSSs in subspace 1 is practical using the method proposed under the variation of time delay for the slack bar power, and the system frequency damping is available. However, the time response is more superior for the respective subspace in the case of adjacent 2 and 3, the system still has damping, which determines that although there is the possibility of classification to a subspace that does not correspond, the system can have a level adequate damping oscillation mode.

In Fig. 13, the case of the highest system load corresponding to subspace ten is presented. The proposed method's effectiveness is observed under the variation of time delay, for

TABLE 4. Regression of subspace – matrix confusion.

Subspace	1	2	3	4	5	6	7	8	9	10
E_1	490	24	0	0	0	0	0	0	0	0
E_2	20	483	18	0	0	0	0	0	0	0
E_3	3	10	481	20	0	0	0	0	0	0
E_4	0	3	22	480	32	4	0	0	0	0
E_5	0	0	0	24	479	20	0	0	0	0
E_6	0	0	0	1	5	476	21	3	0	0
E_7	0	0	0	0	0	14	481	10	0	0
E_8	0	0	0	0	0	0	12	482	15	16
E_9	0	0	0	0	0	0	0	20	489	21
E_{10}	0	0	0	0	0	0	0	0	16	486

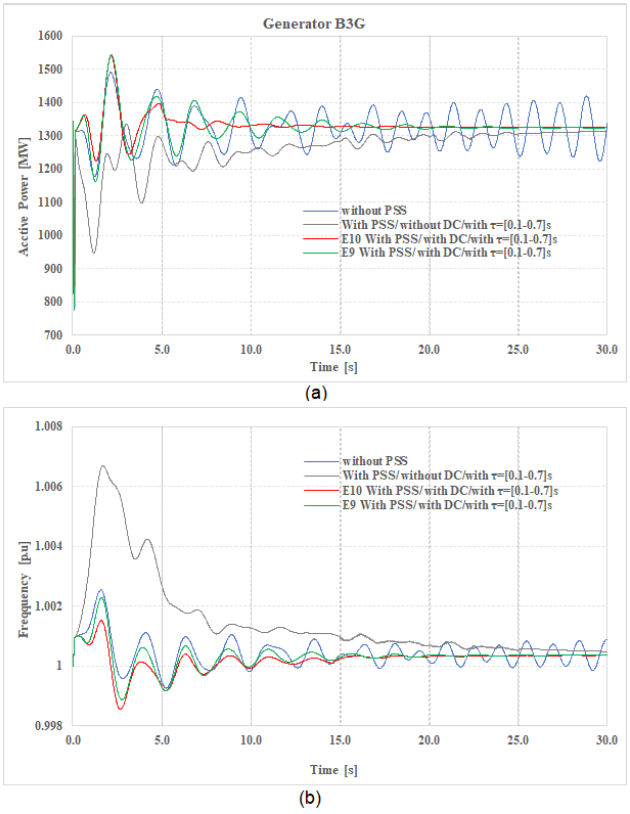

FIGURE 13. Time response of the system under varying time delay in the case of two subspace boundaries. a) response of slack bus. b) frequency of the system.

the slack bar power and the system frequency, even damping is available. However, the response time is higher for the respective subspace than for the adjacent subspace 9, and the system continues with adequate damping.

In this way, the set of tuning parameters of PSSs could be adaptively changed from one to the other subspace without compromising the system's damping. In Fig. 14, the dynamic response is shown considering a time delay of 0.7 seconds, where the dotted curve corresponds to the reaction considering the tuning of the PSSs of subspace five fixed for all simulations, while the solid curve presents the response of the adaptive selection of a set of PSSs according to the operating conditions. In which, a better response of the damping of the

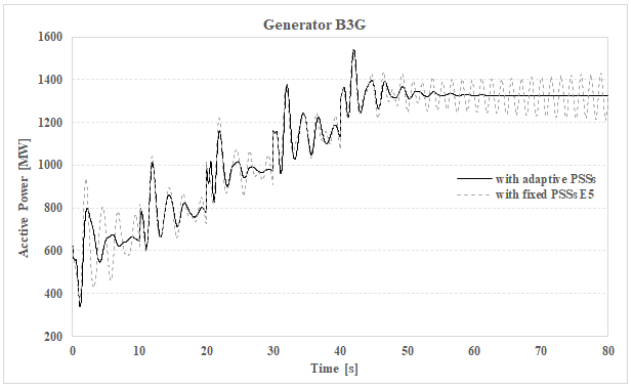

FIGURE 14. Time response of the system under varying conditions operative of the test system.

system is observed when considering the adaptive method of multiple adaptive conditions.

C. ECUADORIAN ELECTRIC SYSTEM

In 2019, the electric system had a maximum demand of 24753.2 GWh, of which hydroelectric plants produced 88.83%, 1.46% from renewable energy sources, 0.02% from interconnections with Colombia and Perú, 9.68% of the energy. That could meet the demand for 2019 was obtained from 123 thermal generation units based on turbo steam, gas, diesel, and internal combustion engines, 150 hydraulic generation units, and 30 renewable generation units (Photovoltaic, wind, and biomass) with power generation installed at 7253 MW, 610.17 km of 500kV and 3199 km of 230 kV transmission lines [26].

To verify the validity of the proposed methodology and as the operating point through which the PSSs are tuned. The operation condition changes, it is necessary to obtain from the WAMS additional to the frequency and power measurements. The measurements of the oscillation modes are obtained (amplitude, damping, and frequency), with which the critical oscillation modes are determined, which in the case of Ecuadorian electrical system electrical network called ''National Interconnected System (SNI)'' corresponds to 7%, as presented in Table 5, with which adequate modeling of the electrical network is determined.

Each of the SNI plants that have PSS is considered the model proposed in the article, and in the case of power plants that have more than one unit, it is considered one plant.

Fig. 15 shows that for the analysis of a real system, the decision tree's optimal number corresponds to eleven subspaces that determine an adequate CART mismatch that reaches 0.0378, representing a 96.2% probability of selecting the correct subspace.

The dynamic response of the Coca Codo Sinclair (CCS) power plant at 1500 MW is displayed in Fig. 16. The dashed curve is the dynamic response of the power plant with the fixed set of PSSs predesigned for subspace 6. The solid curve is the response to the adaptive control method proposed in this paper. From this figure, it can be seen that the adaptive control method shows excellent performance for the operation system.

TABLE 5. Eigenanalysis results.

Mode No.	Eigenanalysis		WAMS	
	Damp (%)	Freq. (Hz)	Damp (%)	Freq. (Hz)
1	6.3286	3.0633	6.421	3.014
2	3.6127	1.1551	3.822	1.095
3	5.3939	1.3541	5.573	1.324
4	6.3879	1.2377	6.427	1.209
5	6.6765	1.1622	6.713	1.156

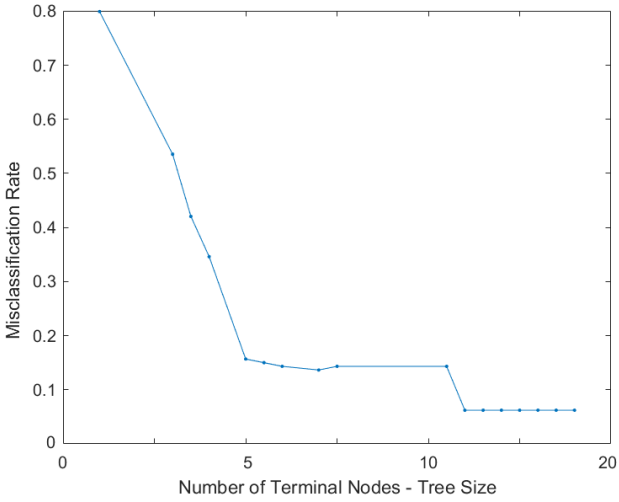

FIGURE 15. The misclassification rate of tree size for SNI.

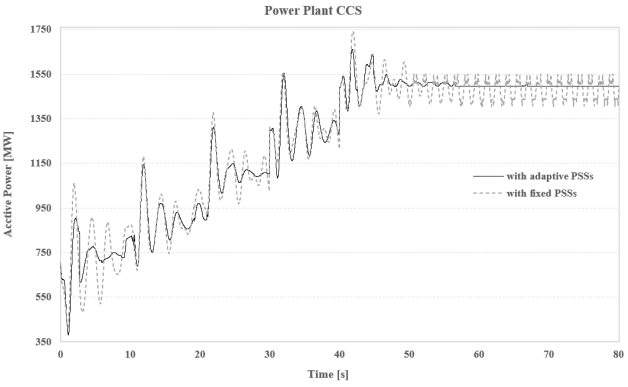

FIGURE 16. Dynamic response of power plant CCS under varying conditions operative.

VI. CONCLUSION

This paper uses a damping control considering stochastic of operating conditions and time delay in WAMS measurements as an additional uncertainty. In this direction, the system's dynamic behavior can be monitored and with an adequate set of PSS tuning parameters, which can be adaptive changed using the existing infrastructure, achieving that the proposed method can accurately assess the effect of two important power systems uncertainties on the system SSS.

Though it uses data management techniques such as CART, the simulation presented can demonstrate the ability to improve small-signals' stability, increasing robustness in the face of varying operating conditions, with which it is possible to extend the operating range of the system. The test results show that the proposed method identified the located and tuning PSS and found other parameters to the general understanding of small-signal stability.

In most tests, DTs built using subspaces give nearly accurate estimations, this shows that the proposed method can select a few of the variables correctly by subspace to reduce the measurement/communication investment, and at the same time, keep good accuracy for small-signal stability.

Therefore, to apply this proposed method in real power systems, it is necessary to collect an adequate sampling of WAMS. Future work might also be performed to provide a comparative assessment of using other optimization tools.

REFERENCES

[1] J. H. Chow and J. J. Sanchez-Gasca, *Power System Modeling, Computation, and Control*, 1st ed. Hoboken, NJ, USA: Wiley, 2020, pp. 149–171.
[2] D. Mondal, A. Chakrabarti, and A. Sengupta, *Power System Small Signal Stability Analysis and Control*, 2nd ed. New York, NY, USA: Academic, 2020, pp. 125–167.
[3] W. Hu, J. Liang, Y. Jing, and F. Wu, "Model of power system stabilizer adapting to multi-operating conditions of local power grid and parameter tuning," *MDPI Sustainability*, vol. 10, no. 6, pp. 2089–2107, Jun. 2018.
[4] E. L. Miotto, P. B. de Araujo, E. de Vargas Fortes, B. R. Gamino, and L. F. B. Martins, "Coordinated tuning of the parameters of PSS and POD controllers using bioinspired algorithms," *IEEE Trans. Ind. Appl.*, vol. 54, no. 4, pp. 3845–3857, Jul. 2018.
[5] L. Cheng, G. Chen, W. Gao, F. Zhang, and G. Li, "Adaptive time delay compensator (ATDC) design for wide-area power system stabilizer," *IEEE Trans. Smart Grid*, vol. 5, no. 6, pp. 2957–2966, Nov. 2014.
[6] S. Gurung, F. Jurado, S. Naetiladdanon, and A. Sangswang, "Comparative analysis of probabilistic and deterministic approach to tune the power system stabilizers using the directional bat algorithm to improve system small-signal stability," *Elsevier Electr. Power Syst. Res.*, vol. 181, no. 1, pp. 171–181, Jan. 2020.
[7] S. Gurung, F. Jurado, S. Naetiladdanon, and A. Sangswang, "Optimized tuning of power oscillation damping controllers using probabilistic approach to enhance small-signal stability considering stochastic time delay," *Electr. Eng.*, vol. 101, no. 3, pp. 969–982, Sep. 2019.
[8] X. Zhang, C. Lu, X. Xie, and Z. Y. Dong, "Stability analysis and controller design of a wide-area time-delay system based on the expectation model method," *IEEE Trans. Smart Grid*, vol. 7, no. 1, pp. 520–529, Jan. 2016.
[9] K. Charles, N. Urasaki, T. Senjyu, M. Lotfy, and L. Liu, "Robust load frequency control schemes in power system using optimized PID and model predictive controllers," *Energies*, vol. 11, no. 11, p. 3070, Nov. 2018.
[10] K. Mansiri, S. Sukchai, and C. Sirisamphanwong, "Fuzzy control for smart PV-battery system management to stabilize grid voltage of 22 kV distribution system in thailand," *Energies*, vol. 11, no. 7, p. 1730, Jul. 2018.
[11] J. A. Oscullo and C. F. Gallardo, "Residue method evaluation for the location of PSS with sliding mode control and fuzzy for power electromechanical oscillation damping control," *IEEE Latin Amer. Trans.*, vol. 18, no. 1, pp. 24–31, Jan. 2020.
[12] R. Majumder, B. Chaudhuri, and B. C. Pal, "A probabilistic approach to model-based adaptive control for damping of interarea oscillations," *IEEE Trans. Power Syst.*, vol. 20, no. 1, pp. 367–374, Feb. 2005.
[13] T. Wang, A. Pal, J. S. Thorp, and Y. Yang, "Use of polytopic convexity in developing an adaptive interarea oscillation damping scheme," *IEEE Trans. Power Syst.*, vol. 32, no. 4, pp. 2509–2520, Jul. 2017.
[14] H. Ye and Y. Liu, "Design of model predictive controllers for adaptive damping of inter-area oscillations," *Int. J. Electr. Power Energy Syst.*, vol. 45, no. 1, pp. 509–518, Feb. 2013.
[15] J. Ma, *Power System Wide-Area Stability Analysis and Control*, 1st ed. Hoboken, NJ, USA: Wiley, 2018, pp. 268–288.
[16] M. Li and Y. Chen, "Designing of power system stabilizer based on neural-like p systems," *Proc. Inst. Mech. Eng., I, J. Syst. Control Eng.*, vol. 234, no. 2, pp. 199–210, Feb. 2020.
[17] E. E. Bernabeu, J. S. Thorp, and V. Centeno, "Methodology for a security/dependability adaptive protection scheme based on data mining," *IEEE Trans. Power Del.*, vol. 27, no. 1, pp. 104–111, Jan. 2012.
[18] R. A. Fisher, "The use of multiple measurements in taxonomic problems," *Ann. Eugenics*, vol. 7, no. 2, pp. 179–188, Sep. 1936.
[19] T. Surinkaew and I. Ngamroo, "Inter-area oscillation damping control design considering impact of variable latencies," *IEEE Trans. Power Syst.*, vol. 34, no. 1, pp. 481–493, Jan. 2019.
[20] W. Michiels, V. Van Assche, and S.-I. Niculescu, "Stabilization of time-delay systems with a controlled time-varying delay and applications," *IEEE Trans. Autom. Control*, vol. 50, no. 4, pp. 493–504, Apr. 2005.
[21] S. A. Campbell and R. Jessop, "Approximating the stability region for a differential equation with a distributed delay," *Math. Model. Natural Phenomena*, vol. 4, no. 2, pp. 1–27, 2009.
[22] M. Liu, I. Dassios, G. Tzounas, and F. Milano, "Stability analysis of power systems with inclusion of realistic-modeling WAMS delays," *IEEE Trans. Power Syst.*, vol. 34, no. 1, pp. 627–636, Jan. 2019.
[23] J. He, X. Wu, P. Li, C. Lu, and J. Wu, "Design and experiment of wide area HVDC supplementary damping controller considering time delay in China southern power grid," *IET Gener., Transmiss. Distrib.*, vol. 3, no. 1, pp. 17–25, Jan. 2009.
[24] J. Rueda, J. C. Cepeda, I. Erlich, A. B. Korai, and F. M. Gonzalez-Longatt, "Probabilistic approach for risk evaluation of oscillatory stability in power systems," in *PowerFactory Applications for Power System Analysis*, 1st ed. New York, NY, USA: Springer, 2014, ch. 11, pp. 249–266.
[25] Eric Siegel, CART. (2019). *Salford Systems*. [Online]. Available: https://www.salfordsystems.com
[26] "ISO CENACE," ISO CENACE, Quito, Ecuador, Annu. Rep., Dec. 2019.

JOSÉ ANTONIO OSCULLO LALA (Student Member, IEEE) received the B.Sc. degree in electrical engineering from the National Polytechnic School, Quito, Ecuador, in 1996, and the M.Sc. degree in electrical engineering from the University of Campinas, Brazil, in 2002. He is currently pursuing the Ph.D. degree in electrical engineering with the National Polytechnic School, Ecuador. His research interests include the modeling, analysis, and simulation of smart grid.

CARLOS FABIAN GALLARDO received the B.Sc. degree in electrical engineering from the National Polytechnic School, Quito, Ecuador, in 1999, and the Ph.D. degree in electrical engineering from University Carlos III, Madrid, in 2009. His research interest includes the electronic power for application in operative system electric power.